RSC Advances

ROYAL SOCIETY OF CHEMISTRY

www.rsc.org/advances

Cyclodextrin facilitated electrospun chitosan nanofibers

Nancy A. Burns[a], Michael C. Burroughs[a], Hanna Gracz[b], Cailean Q. Pritchard[a], Alexandra H. Brozena[a], Julie Willoughby[c], and Saad A. Khan[a1]

[a]Department of Chemical and Biomolecular Engineering, North Carolina State University, Raleigh, NC 27695-7905

[b]Department of Chemistry, North Carolina State University, Raleigh, NC 27695-8204

[c]Department of Textile Engineering, Chemistry, and Science, North Carolina State University, Raleigh, NC 27695-8301

Abstract

The use of chitosan, a cationic biodegradable polysaccharide derived from sea-shells, in nanofibrous form offers a powerful platform to exploit its inherent benefits. However, chitosan nanofiber formation is difficult, requiring corrosive solvents or a carrier polymer blend to successfully electrospin. Our approach entails blending chitosan with a functional small molecule, cyclodextrin, to facilitate nanofiber formation of chitosan in acetic acid and trifluoroacetic acid. In this case the cyclodextrin, with its complexation properties, could serve to improve chitosan fiber formation, thus serving as a multi-functional blend. In this study, we examine the role of each component and the possibility of synergistic effects in nanofiber formation. Significant improvements in chitosan fiber formation were observed in concert with cyclodextrin at solvent concentrations not possible with just the individual components. Multiple fiber morphologies including three-dimensional fiber mats were also achieved. We examine the improved nanofiber formation in relation to solution viscosity, polymer entanglement, and chitosan-cyclodextrin associations. Rheological studies provide evidence of interactions between cyclodextrin and chitosan. NMR and FTIR studies further validate complexation between these two components.

[1] Corresponding author: e-mail khan@eos.ncsu.edu; Ph 919-515-4519

† Electronic supplementary information (ESI) available: Solution conductivity and surface tension measurements are provided, together with SEM images of electrospun samples containing urea.

1. Introduction

The use of chitosan, a cationic biodegradable polysaccharide derived from sea-shells, in nanofibrous form offers a powerful platform to exploit its inherent benefits.[1] The structure of chitosan, consisting of randomly distributed β-(1-4)-linked D-glucosamine (deacetylated) and N-acetyl-D-glucosamine (acetylated) units, contributes to the unique cationic nature and various properties.[2] When the solution pH is below the pK_a, the deacetylated amine groups become protonated. This cationic nature enables chitosan to penetrate mucus layers in biomedical applications, to act as an antimicrobial agent in food preservatives, and to trap metals and dyes in waste water.[2-4] These unique properties of chitosan, combined with the high surface area and porosity of nanofibers have led to the study of several functional systems. For example, Wang *et al.* fabricated formaldehyde sensors from polyethyleneimine functionalized chitosan nanofibers.[5] Alternatively, blended chitosan nanofibers have been examined for water purification by absorbing nickel, cadmium, lead, and copper.[6]

While these nanofiber systems are versatile due to the presence of chitosan, they require either a corrosive solvent or the addition of another polymer to aid in the electrospinning process.[1,7] The addition of another polymer, often called a carrier polymer, is common in chitosan electrospinning literature because chitosan has proven extremely challenging due to several different factors. First, chitosan does not dissolve in common solvents and can only be dissolved at low concentrations in acidic solvents. Second, chitosan is highly crystalline in nature with its rigid structure inhibiting chain entanglement and thus fiber formation.[7] Furthermore, when dissolved in acidic solvents, chitosan will be positively charged due to its polyelectrolyte nature. It is believed that these repulsive charges, in combination with the electrospinning electric field, interfere with uniform fiber formation and instead results in the

production of beads.[1,7] Finally, chitosan is a batch material that is derived from an assortment of natural materials including plant cell walls and anthropoid exoskeletons. The combination of these materials and the different hydrolysis methods used to manufacture chitosan makes it a highly variable product which adversely affects reproducibility of the electrospinning process. The difference in molecular weight and ratios of deacetylated to acetylated groups, or the deacetylation degree (DD%), that exists between different chitosan samples impacts chitosan solubility and polymer chain entanglement.[2]

Despite the previously stated challenges, neat chitosan nanofibers have been successfully electrospun in aqueous acetic acid, trifluoroacetic acid (TFA), and TFA/dichloromethane mixtures.[8-9] However, blending chitosan with a carrier polymer is the typical approach to promote nanofiber formation. And in this regard, chitosan blends with polyethylene oxide, polyvinyl alcohol, polyethylene terephthalate, polyethylene glycol, gelatin, or collagen have been electrospun to obtain nanofibrous mats.[1,10-12] In this study, we take a different approach and use cyclodextrin, a small molecule, to facilitate fiber formation of chitosan.

Cyclodextrins are nontoxic, hollow, truncated oligosaccharides with hydrophilic exteriors and hydrophobic interiors and are of interest due to their unusual hosting abilities. Hosting, or complexation, within cyclodextrin is the non-covalent incorporation of a guest into a protective electron rich cavity.[13] Cyclodextrin's cavity is not only ideal for hosting guests, but can also be used to reorganize polymer structures, morphologies, and even conformations.[14] Our goal is to use this hosting ability of cyclodextrin to coalesce or interact with various polymer chains to facilitate chitosan fiber formation. Incorporation of cyclodextrin into an electrospun nanofiber mat has been achieved.[15-18] However, cyclodextrin incorporation to introduce complexation properties that aid chitosan electrospinning and its effect on fiber formation has yet to be

explored. Therefore, this work focuses on realizing the full potential of chitosan electrospinning by understanding the mechanism that enables fiber formation through complexation as a function of solution properties, solvent types, and cyclodextrin content, and its effect on fiber morphology.

2. Experimental section

Materials

Technical grade hydroxypropyl β-cyclodextrin (HPCD, 5.6 degree of substitution) was purchased from CTD, Inc. (High Springs, FL) and used as received. Chitosan (CS, 75-85% deacetylated), deuterated water, and trifluoroacetic acid (TFA) were purchased from Sigma Aldrich and used as received. Glacial acetic acid (AA) and sodium chloride were purchased from Acros and then diluted to the required volume percent with de-ionized water.

Solution characterization

Solutions were prepared by adding the desired amounts (wt.%) of chitosan and HPCD to the solvent (vol.%). Solutions were mixed overnight in a shaker bath at room temperature. To prevent degradation, chitosan and all solutions were stored at 4°C and used within ten days of initial preparation.

Surface tension measurements, using the Wilhelmy plate method, were done in triplicate to ensure reproducibility. Various concentrations of chitosan and HPCD were examined in different solvent systems to determine the effect of surface tension on fiber formation. Conductivity was measured using a Mettler Toledo meter to determine the effect of solution conductivity on fiber formation. Solution viscosity was measured using a TA Instruments® AR-2000 stress controlled rheometer with a 4 cm, 2° cone and plate geometry and solvent trap. Steady state experiments were run at room temperature for a range of chitosan concentrations

with and without HPCD. The zero shear viscosity (η_o), the viscosity at low shear rates, and the solvent viscosity (η_s) were used to determine the specific viscosity. Reproducibility of the measurements was within ±5% for three separate measurements. Solution characteristics for the TFA solutions were not measured due to their corrosive nature.

^{1}H and ^{13}C NMR spectra were recorded on 700 MHz Bruker Avance III spectrometer operating at 30 °C and 700.17 MHz proton frequency equipped with cryoprobe and Topspin 2.1 software version (Bruker, Karlsruhe, Germany). The NMR probe was tuned to ^{13}C frequency, which is 176.05 MHz in the 700.17 MHz spectrometer. A capillary tube with benzene was used as a ^{13}C external standard (130.3 ppm). All spectra were collected with 90^{o} ^{1}H and ^{13}C standard pulses at a relaxation delay of 2 s and 128 scans. The NMR signal was Fourier transformed without apodization and the phase and baseline were carefully corrected. Assignments of ^{1}H and ^{13}C NMR signals to HPCD and chitosan were made using prediction software ACD (Advance Chemistry Development, Toronto, Ontatrio, Canada) and confirmed by 2D heteronuclear single quantum correlation (HSQC, ^{1}H-^{13}C) NMR experiments.[19] Samples were prepared for NMR spectroscopy by dissolving 2 or 20 wt.% of chitosan or HPCD, respectively, in 90AA/10 D_20 vol.% and transferred to a 5-mm NMR tube for analysis. Tubes were carefully washed and dried for 24 hrs in an oven and bubbled with nitrogen before being capped for storage.

Electrospinning

To electrospin, 1mL of solution was inserted into a 10 mL syringe and fit with a metal needle (0.508 mm I.D.). The syringe was secured to a New Era precision syringe pump (model NE-1010) with a needle tip-to-collector plate distance of 10 cm. Voltage was applied once the solution had equilibrated to a flow rate of 0.3 mL/hr. The voltage was increased slowly (7-13

kV) until the drop of solution at the needle tip formed a Taylor cone and the sample deposited onto the foil covered grounded collector plate.

Fiber characterization

Fiber morphology was examined via scanning electron microscopy (SEM). The samples were coated with a thin layer of gold (approximately 10 nm) and then studied with a FEI XL-30 SEM. Fiber diameters were determined by averaging the measurements of 100 fibers using ImageJ software (NIH). Mat porosity was analyzed using SEM micrographs and ImageJ binary processing. Mat porosity was determined to be the percent of void space area to the total surface area.[20] Data is expressed as mean ± standard deviation (n = 5) with the statistical significance difference determined *via* one-way analysis of variance ($p < 0.1$).

Infrared spectra of electrospun fiber mats and films were measured with an attenuated total reflectance Fourier transform (ATR-FTIR, Nicolet 6700) spectrophotometer equipped with a Ge crystal and purged with dry air. Each spectrum was acquired with 256 scans with a resolution of 4 cm^{-1} and a spectral range of 4000−600 cm^{-1}.

3. Results and discussion

Chitosan/cyclodextrin electrospinning

We begin by blending chitosan with HPCD to promote fiber formation. Electrospinning improvements were observed by the formation of a well-defined Taylor cone, the rapid appearance of fiber deposits on the collector plate, and the formation of a mat that can be removed from the foil and handled due to improved mechanical properties, all of which was not seen with neat chitosan. More importantly, these improvements translate into enhancements in chitosan fiber morphology. As seen in Fig. 1, characteristic electrospinning morphology transitions from beads to beaded fibers and ultimately to uniform fibers with increased HPCD

content. Fiber morphology improvements are not solely due to HPCD's ability to electrospin, but are due to an interaction between chitosan and HPCD. Interestingly, this interaction leads to uniform fiber formation from chitosan/HPCD blends at less than half the required HPCD content of neat HPCD systems.[15]

Uniform fiber formation is not restricted to low chitosan or HPCD concentrations; instead nanofibers can be electrospun using a range of concentrations. This wide range of concentrations leads to tunable mat properties including mechanical strength and dissolution rates (Figs. S1, S2 and Table S1). Controlling the material content also introduces the ability to alter the mat topology. Electrospinning near the chitosan/HPCD solubility limit in TFA results in an interesting mat phenomenon where fibers begin to extend off the collection plate (Fig. 2) and are thus termed three-dimensional (3D) electrospun mats. The mat thicknesses are time dependent, with the thickest region being the center of the mat, causing a conical 3D mat shape to form. The resulting mats are self-supporting after the electrical field is removed. The void space within the mat was found to increase with chitosan content, but did not vary substantially with HPCD content (Fig. S3), suggesting that chitosan plays a role in the 3D phenomenon. Bonino *et al.* reported a similar finding when electrospinning a charged biopolymer system of alginate and polyethylene oxide, and attributed the 3D nature to a combined effect of repulsive charges in alginate and water retention.[21] Interestingly, the formation of our 3D mats seems to depend on high chitosan content. This chitosan dependence supports the charge repulsion theory as increasing the chitosan content increases the charge repulsion and mat porosity. It is possible that a minimum amount of charge repulsion is required before a 3D mat architecture is achieved. Further work is needed to fully probe the mechanism behind chitosan/cyclodextrin 3D mat formation.

In addition to electrospinning at high chitosan concentrations, we are also able to electrospin nanofibers from dilute aqueous acid solvents, such as 1 vol.% AA (Fig. 3). A neat 3 wt.% chitosan solution will not electrospin (Fig. 3a) in dilute AA. However, adding HPCD improves the electrospinnability and ultimately leads to nanofiber formation (Fig. 3d). Electrospinning in dilute acid solvents is significant because it diminishes potential corrosive degradation of active ingredients and reduces the need for post-processing treatments.

Chitosan/cyclodextrin interactions

We examined the electrospinning solution properties to better understand why fiber formation improves with HPCD addition. The addition of HPCD to chitosan solutions reduced the solution conductivity with no appreciable change in surface tension (Fig. S4 and Table S2). Reductions in the solution conductivity typically diminishes the ability to electrospin;[22] however, we observed an improvement in electrospinnability. We believe an increase in solution viscosity may be compensating for the diminished conductivity effect and investigated this further using rheology.

Solution rheology can identify the polymer entanglement concentration and predict the concentrations required for uniform electrospun fibers.[23-24] The polymer entanglement concentration is determined by a slope transition when plotting the specific viscosity ($\eta_{sp} = (\eta_o - \eta_s)/ \eta_s$) as a function of polymer concentration. The slopes from this plot, also known as the scaling exponents, are typically ~ $C^{1.5}$ and $C^{3.8}$ for polyelectrolyte solutions.[25] Shifts in the scaling exponents can indicate changes on a molecular level, with an increase signifying an escalation in polymer association or molecular interactions.[23,26] We have used this method to examine the impact that solvent concentrations and HPCD addition have on the polymer entanglement concentration and interactions. The first step was to establish the scaling

exponents and polymer entanglement concentration of neat chitosan solution as a function of solvent concentration (Fig. 4a). The scaling exponents for neat chitosan in concentrated and dilute AA are similar to each other and to the values reported in literature.[25] This similarity suggests that AA concentration does not significantly change the molecular interactions between chitosan molecules. However, we observe that increasing the AA concentration shifts the polymer entanglement concentration slightly, from 1.8 to 1.3 wt.%, when AA concentration is increased from 10 to 90 vol.%. This shift indicates changes in chitosan chain conformations, with more entanglement at higher AA concentrations. Therefore electrospinning chitosan in concentrated AA leads to uniform nanofibers at lower chitosan concentrations, consistent with what has been observed in the literature.[8] Finally, the impact of HPCD addition on the polymer entanglement concentration and the scaling exponents were analyzed (Fig. 4b). The addition of HPCD did not shift chitosan's entanglement concentration. However, HPCD addition did significantly increase the scaling exponent after the polymer entanglement concentration from $C^{3.8}$ to $C^{7.2}$. This substantial increase suggests that HPCD addition promotes chitosan polymer chain association. A similar increase in scaling exponents ($C^{4.5}$ to $C^{8.0}$) has been seen when poly(alkyl methacrylate) was modified with additional hydrogen bonding groups to improve intermolecular associations between chains.[23]

Improved chitosan interactions or association due to HPCD addition might be due to either hydrogen bonding or complexation of chitosan within HPCD's cavity. Based off the solution rheology results, hydrogen bonding is not believed to play a significant role in fiber formation. If hydrogen bonding was responsible for fiber formation then a reduction of the polymer entanglement concentration would be evident because hydrogen bonding forms extended networks between HPCD and a polymer, as seen in our previous work with HPCD and

a non-complexing polymer, poly(vinyl alcohol).[16] However, there was no polymer entanglement changes in the chitosan/HPCD system. In addition to solution rheology, hydrogen bonding within a solution can be investigated by examining the effect of adding a chaotropic agent to a solution, such as urea. If urea addition affects electrospinnability, then it is possible to conclude that hydrogen bonding plays a significant role in fiber formation.[15] However, we found that urea addition does not impact fiber formation (Fig. S5), indicating that hydrogen bonding is not the primary parameter in chitosan/HPCD electrospinning.

The presence of chitosan within HPCD solutions has been found to impede drug complexation, suggesting that chitosan might be included within or shielding HPCD's cavity.[27] Typical cyclodextrin-guest interactions can be confirmed by examining either the glass transition temperature (T_g) or the crystalline nature.[28] However using calorimetry and crystallography to determine HPCD complexation of chitosan is problematic for two reasons. First, the location of chitosan's T_g is difficult to obtain and highly debated, with literature suggesting that it degrades well before the T_g is reached.[29-30] Second, while most cyclodextrins are crystalline, HPCD is not. In fact, X-ray diffraction patterns of both chitosan and HPCD have undefined, broad, diffused peaks that signify their amorphous nature making reductions in the crystalline nature redundant.[30-31] Therefore, NMR spectroscopy was employed to examining the cyclodextrin proton (^{1}H) chemical shifts ($\Delta\delta$) upon guest addition.[32-33] Unfortunately, a majority of chitosan and cyclodextrin chemical shifts overlap due to their structural similarities, preventing the examination of cyclodextrin chemical shifts. However, we are able to examine how the amine groups in chitosan shift upon HPCD addition using a combination of NMR spectroscopy with 2 wt.% chitosan, 20 wt.% HPCD, and 2/20 wt.% chitosan/HPCD solutions. The carbon spectra of chitosan (Fig. 5a) shows six resonances corresponding to the six carbon atoms in chitosan, with

the deacetylated and acetylated amine carbons represented by severely overlapping chemical shifts at 58.59 and 58.49 ppm (indicated with an asterisk). There is a noticeable shift of these carbon signals to 58.30 and 58.33 ppm when chitosan is blended with HPCD suggesting shielding is occurring. Similar signal shifts corresponding to the amine groups are seen when examining the proton spectra of chitosan and chitosan/cyclodextrin blends (Fig. 5b, indicated with an x). The proton resonances shift downfield from 0.64 and 0.60 ppm to 0.96 and 0.99 ppm respectively, when HPCD is added. This chemical shift is substantial ($\Delta\delta$~0.3ppm) and larger than the typical complexation shift (0.1 ppm).[34-35] The improved resolution in the 2D correlation spectra (Fig. 5c) also show significant shifts of the aromatic amine carbon on chitosan, further emphasizing the impact of HPCD addition. The combination of the carbon and proton chemical shifts and their intensity shows significant interactions occurring between cyclodextrin and chitosan. These interactions obviously include the amine groups in chitosan and may be responsible for the improved chitosan/HPCD fiber formation. Additionally, it is possible that partial complexation is occurring; however, further examination of the cyclodextrin protons are needed to determine how chitosan is positioned and if it is fully included within the cavity of HPCD, a topic for future study.[35-36]

In addition to studying the interactions that might be occurring within the solution, we also examined Fourier transform infrared (FTIR) spectra of electrospun chitosan, HPCD, and chitosan/HPCD nanofiber mats (Fig. 6a) to further understand changes in chitosan interactions or associations due to HPCD addition. All spectra show the presence of –OH, C-H, and C-O stretching at 3500-3100, 2990 and 1164, and 1083cm^{-1}, respectively.[37] The chitosan spectrum shows additional peaks, indicated with an asterisk, at 1650, 1550, and 1408cm^{-1} which represent unreacted acetyl groups on the acetylated section of chitosan and the amines on the deacetylated

section of chitosan.[38] However, these peaks are absent in the chitosan/HPCD mat spectrum, while the -OH, C-H, and C-O peaks still remain. The absence of the acetyl and amine peaks in the chitosan/HPCD mat spectrum suggests that HPCD is interacting with these groups and shielding them from detection, further suggesting an interaction between the amine group and cyclodextrin. In addition, the acetyl and amine group shielding was found to be concentration dependent and occurs in both electrospun mats and films. Films of chitosan with increasing amount of HPCD addition (0, 1, 5, 10, and 20 wt.%) were examined using FTIR-ATR (Fig. 6b). The acetyl and amine peaks were the strongest for neat chitosan, but were also visible for 1 and 5 wt.% HPCD. Increasing HPCD addition to 10 and 20 wt.% resulted in the peaks disappearing. The incremental reduction or absence of these peaks with increasing HPCD content suggests the interaction that is taking place is maximized around 10-20 wt.% HPCD, and supports the possibility of complexation. Similar peak disappearance or shifts in functional groups due to cyclodextrin complexation have been previously reported.[35,39] Furthermore, the extent of complexation depends on the amount of available cyclodextrin, with inclusion interactions increasing with cyclodextrin concentration until all guests are shielded.[32]

4. Conclusions

This study demonstrates that cyclodextrin addition facilitates chitosan fiber formation in a variety of solvent systems and concentrations. The inclusion of cyclodextrin (HPCD) enhanced uniform chitosan based nanofiber formation, and extended the composition and solvent window for nanofiber synthesis while introducing a variety of fiber morphologies. Common electrospinning parameters such as surface tension, conductivity, and viscosity did not fully explain the improved fiber formation; instead, we related the electrospinning improvements to molecular interactions between chitosan and cyclodextrin. Rheological experiments revealed

that the addition of HPCD promoted uniform fiber formation *via* association between HPCD and chitosan without affecting the polymer entanglement concentration. This increase in interaction is believed to be due to the formation of an inclusion complex between chitosan and HPCD. Infrared and NMR results further supported this hypothesis, with both showing significant spectral changes upon HPCD addition, and the participation of the chitosan amine group in the complexation.

References

1. J. D. Schiffman and C. L. Schauer, *Polymer Rev*., 2008, **48**, 317-52.
2. M. Dash, F. Chiellini, R. M. Ottenbrite, and E. Chiellini, *Progress in Polymer Sci.*, 2011, **36**, 981-1014.
3. M. Rhazi, J. Desbrières, A. Tolaimate, M. Rinaudo, P. Vottero, A. Alagui, and M. El Meray, *Eur. Polymer J*., 2002, **38**, 1523-1530.
4. G. Crini and P. Badot, *Progress in Polymer Sci.*,2008, **33**, 399-447.
5. N. Wang, X. Wang, Y. Jia, X. Li, J. Yu, and B. Ding, *Carbohydrate Polymers*, 2014, **108**, 192-199.
6. M. Aliabadi, M. Irani, J. Ismaeili, H. Piri, and M. J. Parnian, *Chemical Engineering J.*, 2013, **220**, 237-243.
7. M. Z. Elsabee, H. F. Naguib, and R. E. Morsi, *Mater. Sci. Eng. C*, 2012, **32**, 1711-26.
8. X. Y. Geng, O. H. Kwon, and J. H. Jang, *Biomaterials*, 2005, **26**, 5427-5432.
9. K. Ohkawa, D. I. Cha, H. Kim, A. Nishida, and H. Yamamoto, *Macromolecular Rapid Communcation*, 2004, **25**, 1600-1605.
10. S. Haider, W. A. Al-Masry, N. Bukhari, and M. Javid, *Polymer Engineering and Science*, 2010, **50**, 1887-1893.
11. Z. Chen, X. Mo, C. He, and H. Wang, *Carbohydrate Polymers*, 2008, **72**, 410–418.
12. H. Zheng, Y. Du, J. Yu, R. Huang, and L. Zhang, *J. of Applied Polymer Sci.*, 2001, **80**, 2558-2565.
13. M. E. Davis and M. E. Brewster, *Nature Reviews Drug Discovery*, 2004, **3**, 1023-1035.
14. A. E. Tonelli, *Polymer*, 2008, **49**, 1725-1736.
15. J. Manasco, C. Saquing, C. Tang, and S. A. Khan, *RSC Adv*., 2012, **2**, 3778-3784.
16. J. L. Manasco, C. Tang, N. A. Burns, C. D. Saquing, and S. A. Khan, *RSC Adv.*,2014, **4**, 13274-13279.
17. A. Celebioglu and T. Uyar, *Langmuir*, 2011, **27**, 6218-26.
18. A. Celebioglu and T. Uyar, *Nanoscale*, 2012, **4**, 621-31.
19. L. Kay, P. Keifer, and T. Saarinen, *J. of American Chem. Soc.*, 1992, **114**, 10663-10665.
20. J. Rnjak-Kovacina, S. Wise, Z. Li, P. Maitz, C. Young, Y. Wang, A. Weiss, Biomaterials, 2011, **32**, 6729-6736.
21. C. A. Bonino, K. Efimenko, S. I. Jeong, M. D. Krebs, E. Alsberg, and S. A. Khan, *Small*, 2012, **8**,1928-36.
22. D. Li and Y. N. Xia, *Advanced Materials*, 2004, **16**, 1151-1170.
23. M. G. McKee, C. L. Elkins, and T. E. Long, *Polymer*, 2004, **45**, 8705-8715.
24. C. Tang, C. D. Saquing, J. R. Harding, and S. A. Khan, *Macromolecules*, 2010, **43**, 630-637.

25. R. Colby, *Rheologica Acta*, 2010, **49**, 425-442.
26. R. J. English, H. S. Gulati, R. D. Jenkins, and S. A. Khan, *J. of Rheology*, 1997, **41**, 427-44.
27. P. Mura, G. Corti, F. Maestrelli, and M. Cirri, *J. Incl. Phenom. Macrocycl. Chem.*, 2007, **59**, 307-313.
28. L. Huang, E. Allen, and A. E. Tonelli, *Polymer*, 1999, **40**, 3211-3221.
29. L. S. Guinesi and E. T. G. Cavalheiro, *Thermochimica Acta*, 2006, **444**, 128-133.
30. P. Dhawade and R. N. Jagtap, *Advances in Applied Sci. Research*, 2012, **3**, 1372-1382.
31. S. Baboota, M. Dhaliwal, and K. Kohli, *AAPS Pharm. Sci. Tech.*, 2005, **6**, 83-90.
32. F. B. T. Pessine, A. Calderini, and G. L. Alexandrino, *Intech*, 2012, **12**, 1-29.
33. H. Dodziuk, W. Kozminski, and A. Ejchart, *Chirality*, 2004, **16**, 90-105.
34. H. J. Schneider, F. Hacket, V. Rüdiger, and H. Ikeda, *Chemical Reviews*, 1998, **98**, 1755-1786.
35. X. Wen, F. Tan, Z. Jing, and Z. Liu, *J. of Pharmaceutical & Biomedical Analysis*, 2004, **34**, 517-523.
36. R. Gelb, L. Schwartz, B. Cardelino, H. Fuhrman, R. Johnson, and D. Laufer, *J. American Chem. Soc.* 1981, **103**, 1750-1757.
37. M. Parabaharan and R. Jayakumar, *International J. of Biological Macromolecules*, 2009, **44**, 320-325.
38. B. Duan, C. H. Dong, X. Y. Yuan, and K. D. Yao, *J. of Biomaterials Sci.*, 2004, **15**, 797-811.
39. D. Wang, C. Ouyang, Q. Liu, H. Yuan, and X. Liu, *Carbohydrate Polymers*, 2013, **93**, 753-760.

Figures

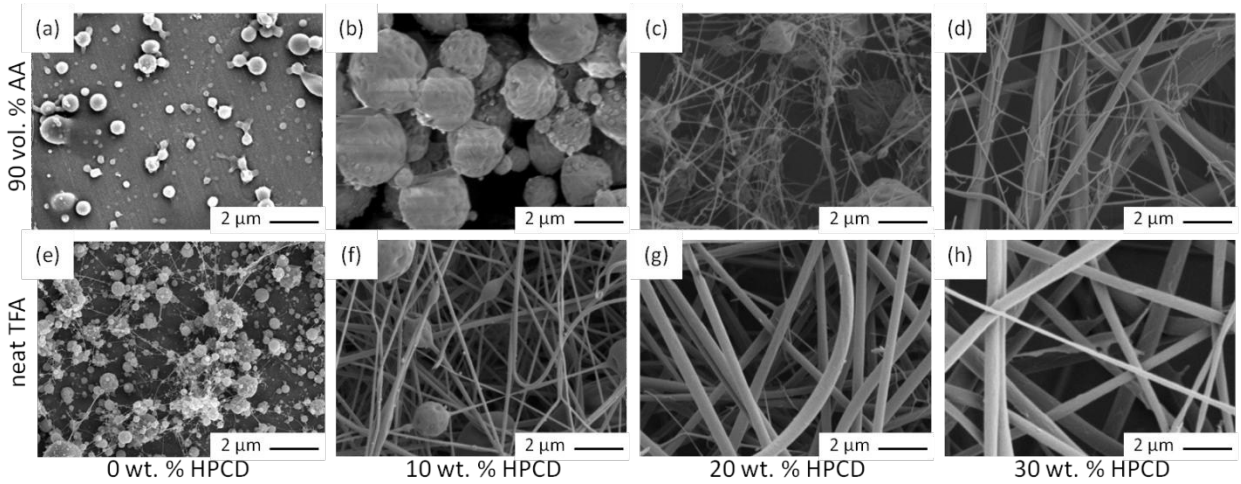

Fig. 1 Fiber morphology of 2 wt.% chitosan in 90 vol.% AA (a-d) and neat TFA (e-h) electrospun mats improves with increasing HPCD content, from (a,e) 0 wt.% HPCD, (b,e) 10 wt.% HPCD, (c,g) 20 wt.% HPCD, and (d,h) 30 wt.% HPCD.

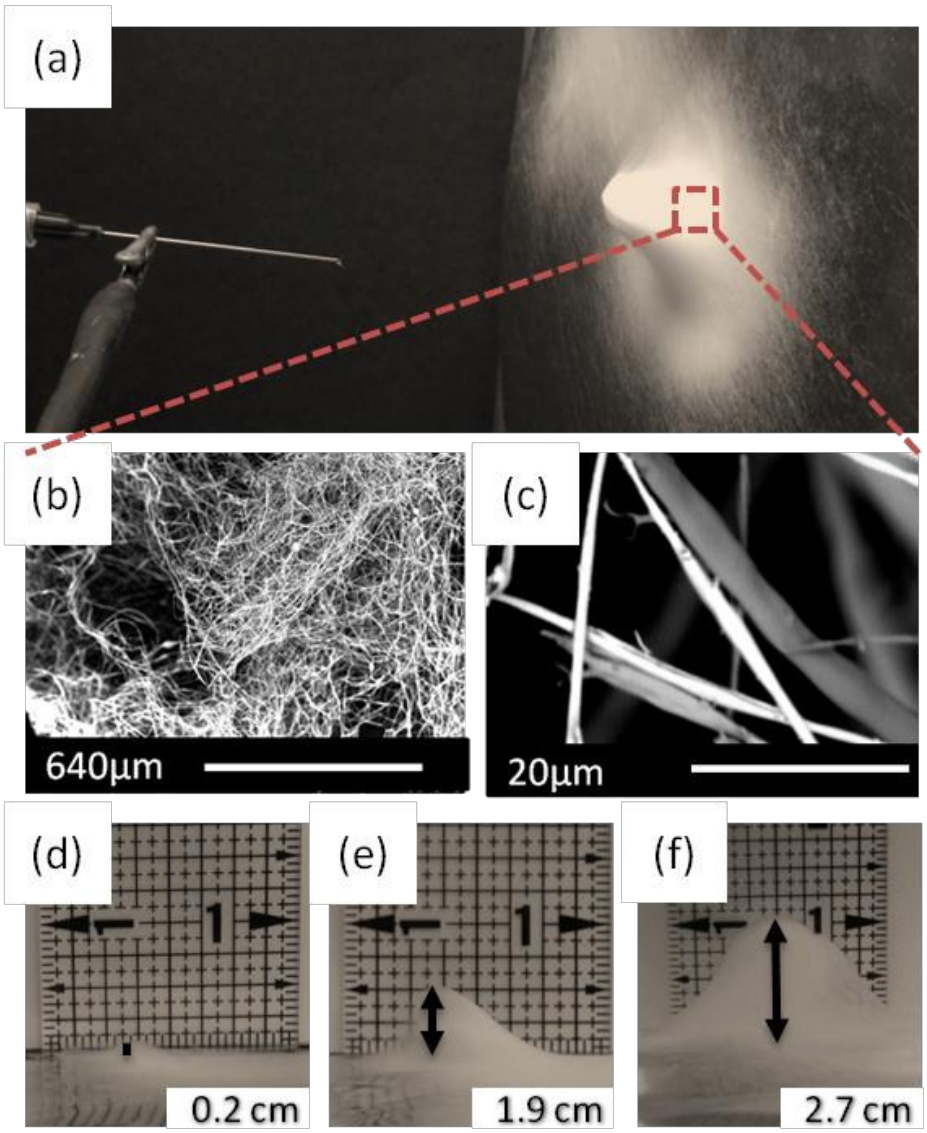

Fig. 2 Three-dimensional (3D) electrospun mats of 4 wt.% chitosan/20 wt.% HPCD/TFA: (a) electrospinning process, (b-c) scanning electron micrographs of a mat section, and mat thickness after electrospinning for (d) 1, (e) 10, and (f) 30 minutes.

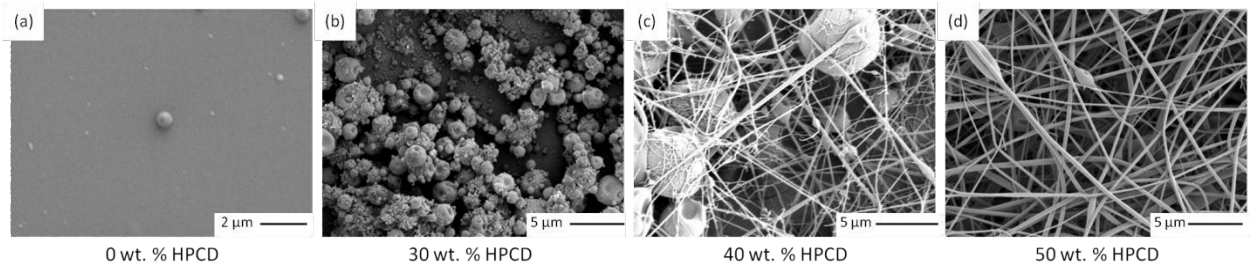

Fig. 3 Fiber morphology of 3 wt.% chitosan electrospun mats in 1 vol.% AA improves with increasing HPCD content: (a) 0 wt.% HPCD, (b) 30 wt.% HPCD, (c) 40 wt.% HPCD, and (d) 50 wt.% HPCD.

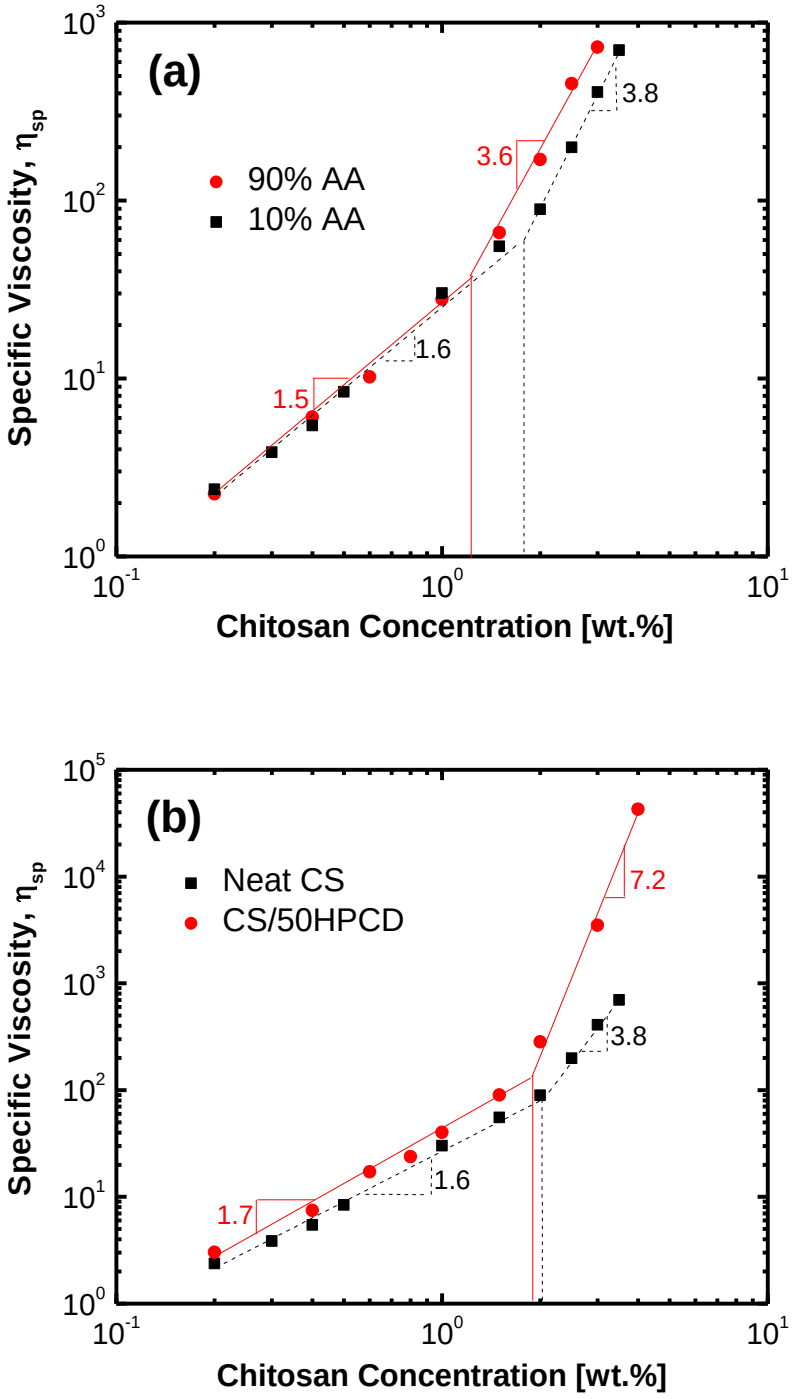

Fig. 4 (a) Solutions dynamics of neat chitosan solutions in 90 vol.% AA (circles) and 10 vol.% AA (squares). (b) Solution dynamics of chitosan solutions in 10 vol.% AA both neat (squares) and blended with 50 wt.% HPCD (circles). The polymer entanglement concentrations, indicated with vertical lines, are effected by solvent choice, while the slopes are increased by HPCD addition.

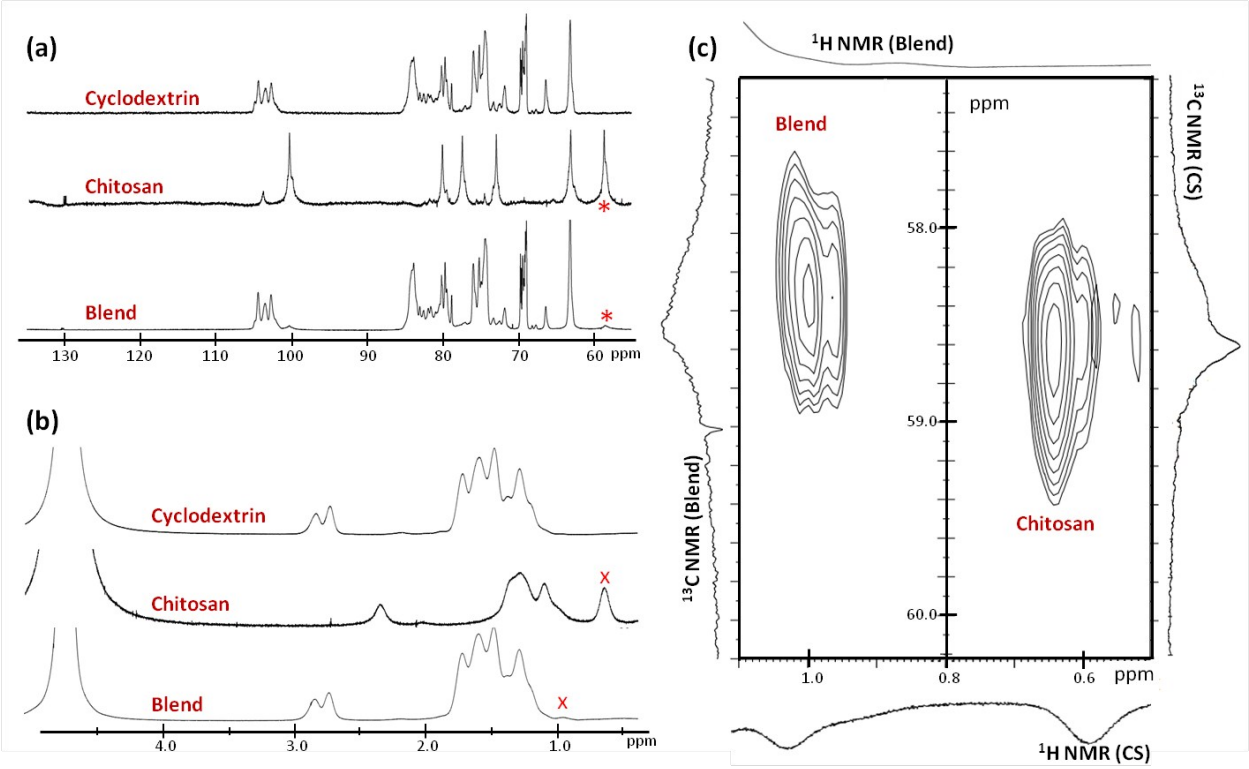

Fig. 5 NMR spectra of 20 wt.% HPCD, 2 wt.% chitosan, and 2/20 wt.% (chitosan/HPCD) blend solutions in 90 vol.% AA and 10 vol.% D_20. The amine carbons and hydrogens are indicated with an asterisk and x, respectively, and shift when blended with HPCD. (a) ^{13}C NMR spectra from top to bottom, HPCD, chitosan, and blend, (b) ^{1}H NMR spectra from top to bottom, HPCD, chitosan and blend, (c) expanded 2D HSQC (^{1}H-^{13}C) NMR spectra contour plot of the blend and chitosan (*top* = ^{1}H NMR of the blend, *bottom* = ^{1}H NMR of chitosan, *left* = ^{13}C NMR of the blend, *right* = ^{13}C NMR of chitosan.)

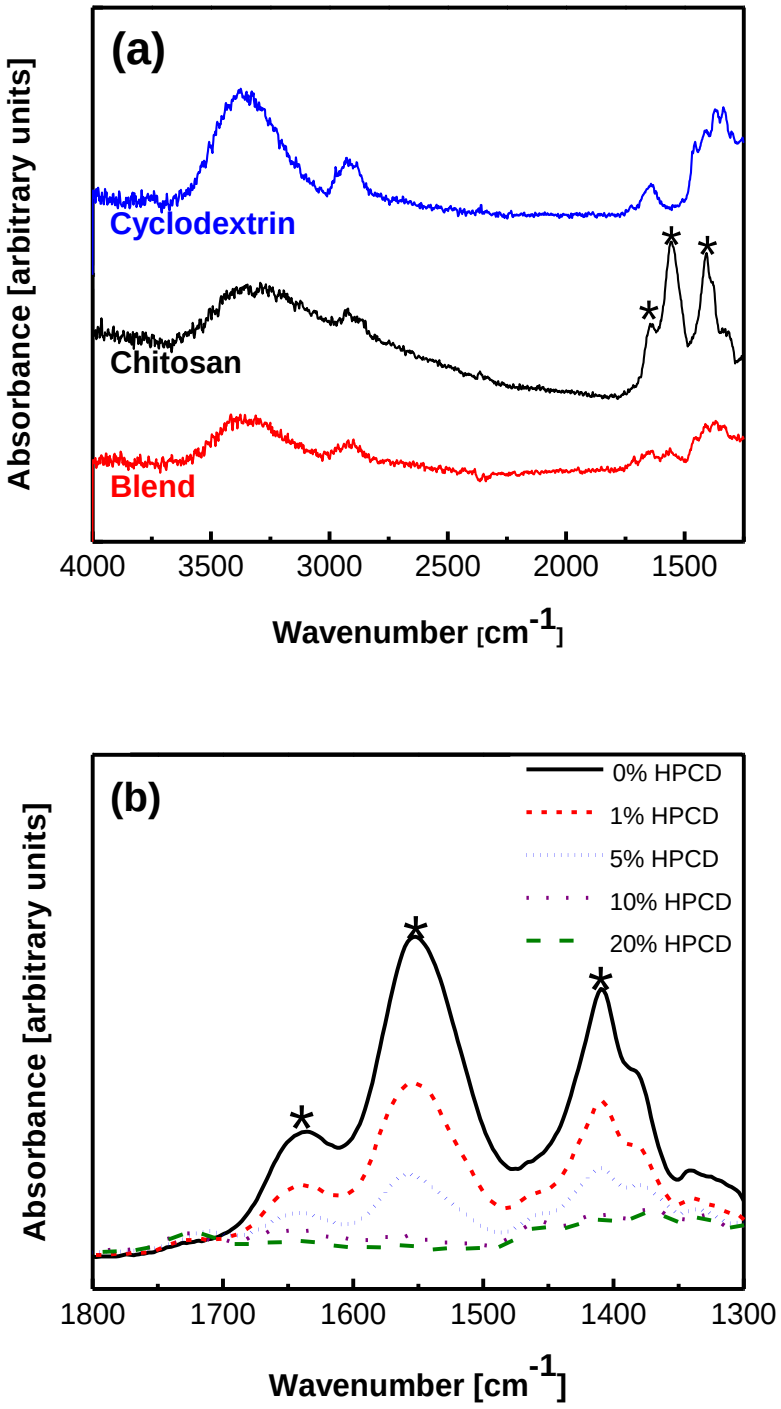

Fig. 6 FTIR spectra in the attenuated reflectance mode of (a) 3 wt.% chitosan, 30 wt.% HPCD, and blended chitosan/HPCD (3/30 wt.%) electrospun mats and (b) films of 2 wt.% chitosan with 0, 1, 5, 10, and 20 wt.% HPCD. Significant chitosan peaks are marked with asterisks and disappear when blended with HPCD.